Crustal Strain in the Marmara Pull-Apart Region Associated With the Propagation Process of the North Anatolian Fault

Ç Karakaş, R. Armijo, R. Lacassin, J.-P Suc, M. Melinte-Dobrinescu

AGU100 ADVANCING EARTH AND SPACE SCIENCE

Tectonics

RESEARCH ARTICLE
10.1029/2017TC004636

Key Points:
- Structural map and geological cross section of the Ganos-Gelibolu fold system in the Dardanelles region
- Timing and amount of shortening associated to the propagation of the North Anatolian Fault are deduced from mapping and critical revision of the stratigraphy
- A tectonic reconstruction of the westward propagation of the NAF in the Dardanelles region is proposed

Supporting Information:
- Supporting Information S1

Correspondence to:
Ç. Karakaş,
ckarakas@ntu.edu.sg

Citation:
Karakaş, Ç., Armijo, R., Lacassin, R., Suc, J.-P., & Melinte-Dobrinescu, M. C. (2018). Crustal strain in the Marmara pull-apart region associated with the propagation process of the North Anatolian Fault. *Tectonics*, *37*, 1507–1523. https://doi.org/10.1029/2017TC004636

Received 21 APR 2017
Accepted 4 APR 2018
Accepted article online 20 APR 2018
Published online 24 MAY 2018

Crustal Strain in the Marmara Pull-Apart Region Associated With the Propagation Process of the North Anatolian Fault

Ç. Karakaş[1,2], R. Armijo[1], R. Lacassin[1], J.-P. Suc[3], and M. C. Melinte-Dobrinescu[4]

[1]Institut de Physique du Globe de Paris, Sorbonne Paris Cité, Université Paris Diderot, Paris, France, [2]Now at the Earth Observatory of Singapore, Nanyang Technological University, Paris, Singapore, [3]Sorbonne Universités, UPMC Université Paris 06, CNRS, Institut des Sciences de la Terre Paris, Paris, France, [4]National Institute of Marine Geology and Geo-ecology GEOECOMAR, Bucharest, Romania

Abstract Propagation processes of plate-scale faults through continental lithosphere are poorly documented. The North Anatolian Fault (NAF) is a continental right-lateral transform with striking evidence for propagation processes in the Marmara Sea pull-apart region. Earlier work (Armijo et al., 1999, https://doi.org/10.1130/0091-7613(1999)027<0267:WPOTNA>2.3.CO;2) suggests that in the Dardanelles, where the principal, northern branch of that fault (NNAF) enters into the Aegean: (1) a fold-thrust system has progressively developed above the NNAF fault tip, at the WSW corner of the Marmara Sea pull-apart. The main anticline formed there was sheared and its SW half laterally offset by ~70 km to the SW; (2) the timing of structure development appears correlated with sea level changes associated with the Messinian Salinity Crisis. Our new description of the Dardanelles (or Ganos-Gelibolu) fold-thrust system is based on structural mapping, field observations, and calcareous nannoplankton analyses to date key sedimentary units. Our results provide tight constraints on the main pulse of folding associated with propagation of the tip of the NNAF: it took place in the late Miocene to earliest Pliocene (5.60 to 5.04 Ma), before deposition of undeformed Pliocene marine sediments. The folding is mostly coeval with the Messinian Salinity Crisis and accommodated several kilometers of shortening at the fault tip. After full propagation of the NNAF up to the surface, the folded structure was sheared and right laterally offset, with an average 14 mm/year of slip rate during the past ~5 Myrs. A reconstruction of tectonic evolution suggests a flower structure nucleating and taking root at the tip of the fault.

1. Introduction

Studying propagation processes of continental plate-scale strike-slip faults over geological timescales (10^5 to 10^7 years) is crucial for our understanding of the mechanical behavior of the lithosphere. The steady deformation process associated with established transform plate boundaries such as the San Andreas Fault (e.g., Bilham & King, 1989; Wilcox et al., 1973) and the New Zealand Alpine Fault (e.g., Roberts, 1995; Walcott, 1978) has been documented extensively. Yet little satisfactory observations document the transient deformation associated with the rapid evolution and propagation of nascent plate boundaries.

The right-lateral North Anatolian Fault (NAF) appears to be an exceptional example of a continental strike-slip fault rapidly evolving into a transform plate boundary within the context of the continental extrusion of the Anatolian Plateau and the Aegean (Flérit et al., 2004). However, in contrast with major strike-slip faults controlling a similar extrusion process in Asia (Tapponnier et al., 1982), the NAF has left unique structural and stratigraphic markers of its growth by propagation from eastern Anatolia to the north Aegean and the Hellenic subduction zone (Armijo et al., 1999).

It is generally accepted that the NAF initiated at the Karlıova triple junction about ~10–13 Myrs ago (Armijo et al., 1996, 1999; Barka, 1992; Şengör et al., 1985) and has grown by westward propagation over its nearly 2,000-km-long trace (Figure 1a; Armijo et al., 1999). It has also been suggested that the propagating tip of the NAF reached the Corinth rift system in Greece around ~1 Ma (Armijo et al., 1996, 1999). Whether the westward propagation of the NAF is driven by the Arabia-Eurasia convergence and Anatolian block extrusion or by slab-pull mechanism associated with the Hellenic subduction zone (or by a combination of both processes) is subject of debate (e.g., Armijo et al., 2003; Flérit et al., 2004; Sternai et al., 2014).

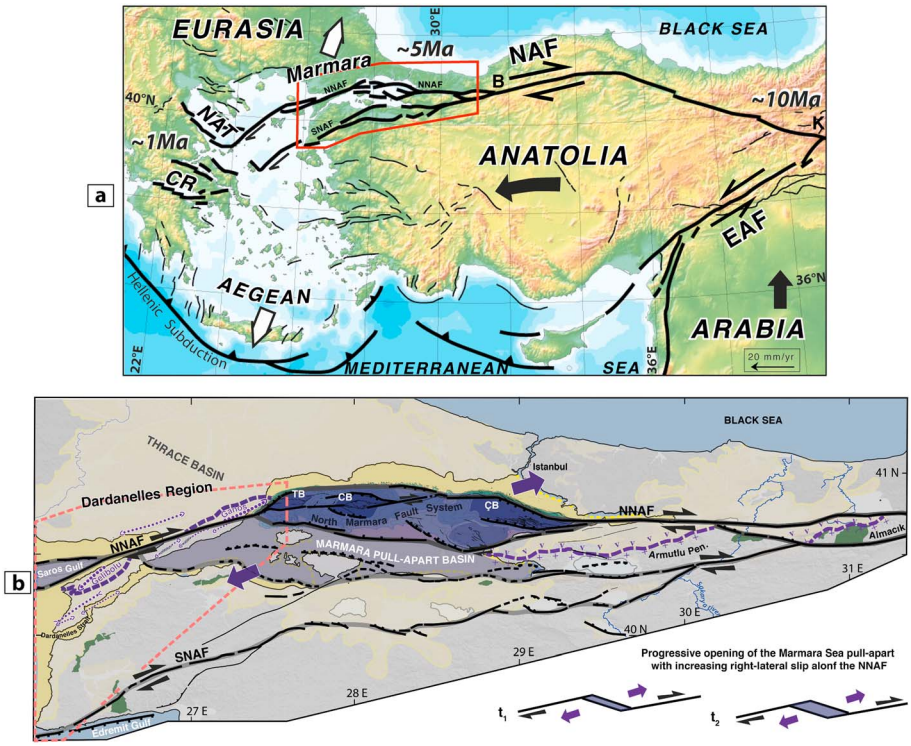

Figure 1. (a) Tectonic framework of continental extrusion in eastern Mediterranean. NAF: North Anatolian Fault; EAF: East Anatolian Fault; NAT: North Aegean trough; CR: Corinth rift; K: Karlıova; B: Bolu. Red box is the area of study. Anatolia is extruded away from Arabia-Eurasia collision and toward the Hellenic subduction zone by displacement along the NAF and EAF. (b) Setting of the two imbricated basins: The Marmara pull-apart basin (purple tones) overprinting the Thrace Basin (yellowish tones). In eastern Sea of Marmara, the E-W NAF cuts and offsets the contact (dashed purple line) nearly coincident with the Intra-Pontide Suture Zone (dislocated blocks of ophiolitic mélange, green) between the Sakarya metamorphic rocks (+) and Eocene volcanics (v) in the Armutlu Peninsula and the Almacık block (Yılmaz et al., 1997). The North Anatolian Fault splays into two main branches (NNAF and SNAF) forming the larger pull-apart (highlighted in light purple, faults redrawn from Armijo et al. 2002). A smaller pull-apart called the north Marmara fault system (dark purple) where most of the lateral motion is accommodated connects the deepest basins (TB: Tekirdağ Basin; CB: Central Basin; and ÇB: Çınarcık Basin) in northern Marmara with two large on land strike-slip faults (E-W NNAF east and NE-SW NNAF west of the Sea of Marmara). The sketch, in right corner (bottom), shows progressive opening (with $t_2 > t_1$) of the pull-apart of Marmara with increasing right-lateral slip on the NNAF.

Studies of geological and geomorphological offsets (Akbayram et al., 2016; Armijo et al., 1999; Barka, 1992; Hubert-Ferrari et al., 2002; Koçyiğit, 1989; Şengör et al., 2005), at different scales along the NAF, allowed identification of markers of fault propagation and estimation of the total displacement on the fault and values of average slip rates over the long term (10^4 years to some 10^6 years). Those estimates are consistent with present-day, nearly instantaneous, estimates from geodetic data (Global Positioning System [GPS], interferometric synthetic aperture radar; Kahle et al., 1998; McClusky et al., 2000, Wright et al., 2001). Both data sets show that most of the deformation between Anatolia and Eurasia is accommodated along the NAF or very close to it. In addition to the large-scale observations mentioned above, modeling of NAF propagation using Coulomb stress failure (Hubert-Ferrari et al., 2003) has emphasized the necessity of considering preexisting lithospheric heterogeneities to understand the propagation processes. Direction of propagation and fault localization would be significantly dependent of defects in the lithosphere. The Marmara Sea pull-apart region (Figures 1a and 1b) is a favorable large-scale area to address crustal structural evolution during the propagation processes of the NAF.

In this work, we test the hypothesis of fault propagation and progressive localization of crustal strain in the Dardanelles (proposed earlier by Armijo et al., 1999) by exploring and documenting in further detail the late Miocene fold system that has apparently formed by shortening while it was placed above of the propagating tip of the NAF. According to the same hypothesis, increasing subsequent slip on the NAF has right-laterally offset the late Miocene fold system, by about 70 km. Here we focus on better characterizing the link

between the NAF and the structures on both sides of it, combining three approaches: (1) we analyze accurately the geology and morphology of Mount Ganos and Gelibolu Peninsula using a high-resolution digital elevation model (DEM, with 30 m resolution), satellite imagery, and field observations, allowing us to build detailed maps and cross sections across the structures clarifying the relationships between sedimentary units; (2) we revise the stratigraphy of sedimentary units by research of calcareous nannofossils, characterized by disappearance and appearance of several species during the time interval 7–4 Ma (middle Miocene to early Pliocene) encompassing the Messinian Salinity Crisis (MSC; 5.97–5.46 Ma; Bache et al., 2012; CIESM, 2008; Manzi et al., 2013) that left clear evidence of its impact in the Dardanelles (Melinte-Dobrinescu et al., 2009). That evidence allows us to determine the timing of compressional deformation; (3) we propose a composite cross section reconstructing the possible geometry of the folded structures on both sides of the NAF prior to their right-lateral offset. That reconstruction allows us to estimate total shortening and average shortening rate in this area, which we compare with geological and present slip rate on the NAF. Finally, we summarize geological, morphostructural, and stratigraphic evidence to construct a 3-D evolutionary model that allows us to describe the process of fault localization and its evolution during fault propagation.

2. Geologic Setting

The Marmara pull-apart region is a structural low between the Black and Aegean Seas marked by superposition of two distinct basins filled with datable continental and marine sediments (Figures 1a and 1b): (1) the Tertiary Thrace Basin (Eocene-Pliocene age) sealing the Intra-Pontide Suture Zone (IPSZ) welding two continents together (Sakarya and Rhodope-Pontide; Turgut et al., 1991; Tüysüz et al., 1998) overprinted on its southern margin by (2) the Pliocene-Quaternary Marmara pull-apart basin, which appears to be closely associated with right-lateral displacement across the NAF (Figure 1b). To the east of the Marmara pull-apart (Figures 1a and 1b), the EW striking nearly linear NAF coming from Central Anatolia splays westward into two main branches (north NAF and south NAF, hereafter designated as NNAF and SNAF) before entering the more diffusely deforming Aegean with a NE-SW direction (Figures 1a and 1b). Changes in strike and segmentation of the NAF within the Marmara pull-apart region cause development of restraining and releasing bends, as well as slip partitioning, so that deformation is distributed in faults and at bends combining strike-slip with normal—or with reverse slip—depending on the nature of the bend (Armijo et al., 2002, 2005; Seeber et al., 2004). Both, kinematic reconstruction of large-scale, long-term geological offsets (of up to ~85 km, over the past ~5 Myrs; Armijo et al., 1999, 2002) and present-day motion determined with GPS data suggest that slip partitioning across the Marmara pull-apart has concentrated on the NNAF about 70–90% of the total motion (Flerit et al., 2003).

The sediment accumulated in the built-in depression of the Sea of Marmara pull-apart basin reaches a thickness in excess of 6 km in the northernmost (e.g., Laigle et al., 2008) and deeper basin that is closely associated with the NNAF (the North Marmara Fault System as in Armijo et al., 2002, Figure 1b). Those sediments are cut by north and south dipping faults with significant normal component of slip, as observed in high-resolution bathymetric maps (Armijo et al., 2002, 2005; Le Pichon et al., 2001), deep-penetration seismic reflection and refraction data (Bécel et al., 2009, 2010; Carton et al., 2007; Laigle et al., 2008; Parke et al., 1999; Wong et al., 1995), and 2-D and 3-D high-resolution multichannel seismic data (Grall et al., 2012, 2013; Kurt et al., 2013). At odds with the evidence for structural complexity and fault segmentation that appear to be fundamental features of the pull-apart system, Imren et al. (2001), Le Pichon et al. (2001, 2003) and Şengör et al. (2005), among others, have alternatively interpreted the Marmara pull-apart system as a trough resulting mainly from the western Anatolia N-S extensional regime during the middle Miocene. The present course of the NNAF would have localized as a single, through-going strike-slip fault, with a "principal displacement zone" that would have initiated within a few 10^5 years (Le Pichon et al., 2001) or sometime after 2.5 Ma (Le Pichon et al., 2016). These authors designate the NNAF as the Main Marmara Fault.

On the northwest edge of the Marmara pull-apart, the NE-SW striking NNAF cuts the southernmost part of the Tertiary Thrace Basin and forms a bend with the North Marmara Fault System (Figures 1b and 2). The NNAF nearly coincides here with the IPSZ (Armijo et al., 1999). North of the NNAF, the tightly folded Eocene-Oligocene sediments of Mount Ganos abut the NNAF obliquely to the north (Figures 1b and 2a). South of the NNAF, similarly folded pre-Tertiary, Eocene-Oligocene, and Miocene and Pliocene sediments are found east of the Saros Gulf and south of it on the Gelibolu Peninsula (Figure 2a). Armijo et al. (1999) associated compressional strain here to a restraining bend at the tip of the westward propagating NAF (Figure 2).

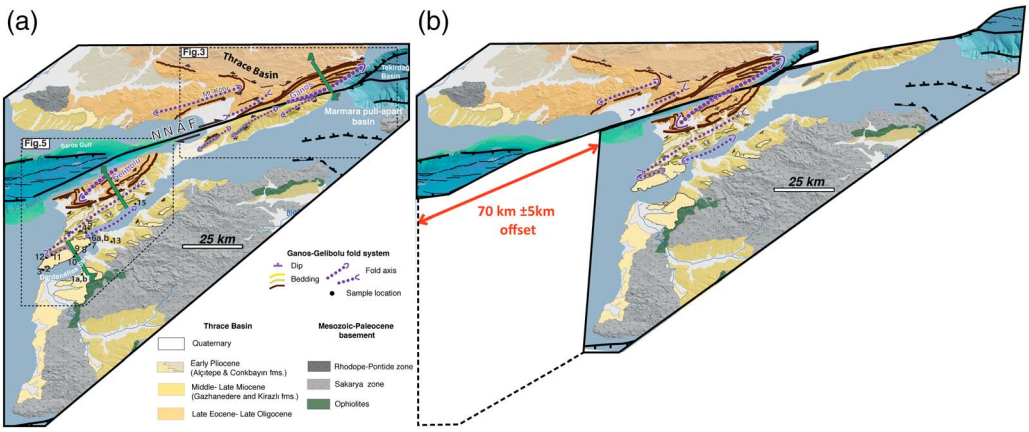

Figure 2. (a) Offset of the Ganos-Gelibolu fold system. Geologic map modified after Armijo et al. (1999) superimposed on a 30 m resolution digital elevation model Centre nationale d'études spatiales (CNES), incentive for the scientific use of images from the spot system) merged with 90 m Shuttle Radar Topography Mission digital elevation model, and the Marmara bathymetry is extracted from the EM300 bathymetry (Rangin et al., 2001); the Saros gulf bathymetry is extracted from Gökaşan et al. (2010). Green lines are location of the composite cross section in Figure 8. *See Table S1 for sample locations.* (b) Reconstructed geometry of the Ganos-Gelibolu Anticline preceding the NAF propagation.

Armijo et al. (1999) identified a possible match between two truncated half-anticlines, affecting Eocene sediments north (Mount Ganos) and south (Gelibolu Peninsula) of the NAF, by restoring ~ 70 km of right-lateral offset (Figure 2). Folding thus would have preceded the onset of right-lateral slip on the NAF across the Gelibolu Peninsula. This suggests that distributed deformation took place within a ~30-km-wide zone, above the NNAF fault extremity prior to its propagation all the way to the surface. The nature and offset of the deformed structures, their relation with the NAF, and the timing of the onset of the fault in the Dardanelles have been questioned by various studies (Le Pichon et al., 2001; Okay et al., 2000, 2004, 2010; Rangin et al., 2004; Yaltırak et al., 2000; Zattin et al., 2005). We address these questions with new observations and age constraints for the Dardanelles fold system.

3. Folding Associated to the NAF Propagation in the Dardanelles (Çanakkale Region)

According to Armijo et al. (1999, 2000), the timing of folding, tightly constrained by an unconformity between the strongly folded strata of middle-late Miocene age (Ghazhanedere and Kirazlı Formations) and the overlying, nearly horizontal marine layers of early Pliocene age (Alçıtepe Formation), (Figures 1b and 2a), occurred during the MSC (Hsü et al., 1973) and the following marine reflooding around ~5.4 Ma.

3.1. Mount Ganos: A Prominent Half-Anticline North of the NAF

Mount Ganos (924 m) and Mount Koru (726 m) are two singular topographic features where basal Eocene-Oligocene sediments of the Thrace Basin outcrop (Figures 1b, 2a, and 3). Both features are anticlines characterized by a nearly intact dome shape and an average trend N45°E oblique to the NAF (N70°E strike). They consist of folded sediments of essentially turbiditic nature alternating with silts, sandstones, andesitic tuffs, and basaltic lavas deposited in a prodeltaic environment (Yaltırak et al., 2000) with a total thickness of ~5.5 km.

Two distinctive observations on the Ganos Anticline allow us to define the overall geometry of the structure and of bedding with respect to the trace and strike of the NAF: (1) Eocene-Oligocene unit dips are gentle close to the core of the structure and to the NAF (25°–40°NW; Figure 4 sections AA′ and BB′). They steepen (40°–68°NW) in the northern flank toward the northeastern tip of the structure (NE of Gaziköy; Figures 3 and 4, section CC′). Secondary smaller-scale recumbent folds with locally fault parallel hinge lines (Okay et al., 2004) are present, mostly within the fold tip region, and Eocene-Oligocene layers turn and form a fold closure. The NNAF obliquely truncates the southwestern end of the folded layers, with the fold axis forming an acute angle with the fault of a ~17 ± 3° (Figure 3a).

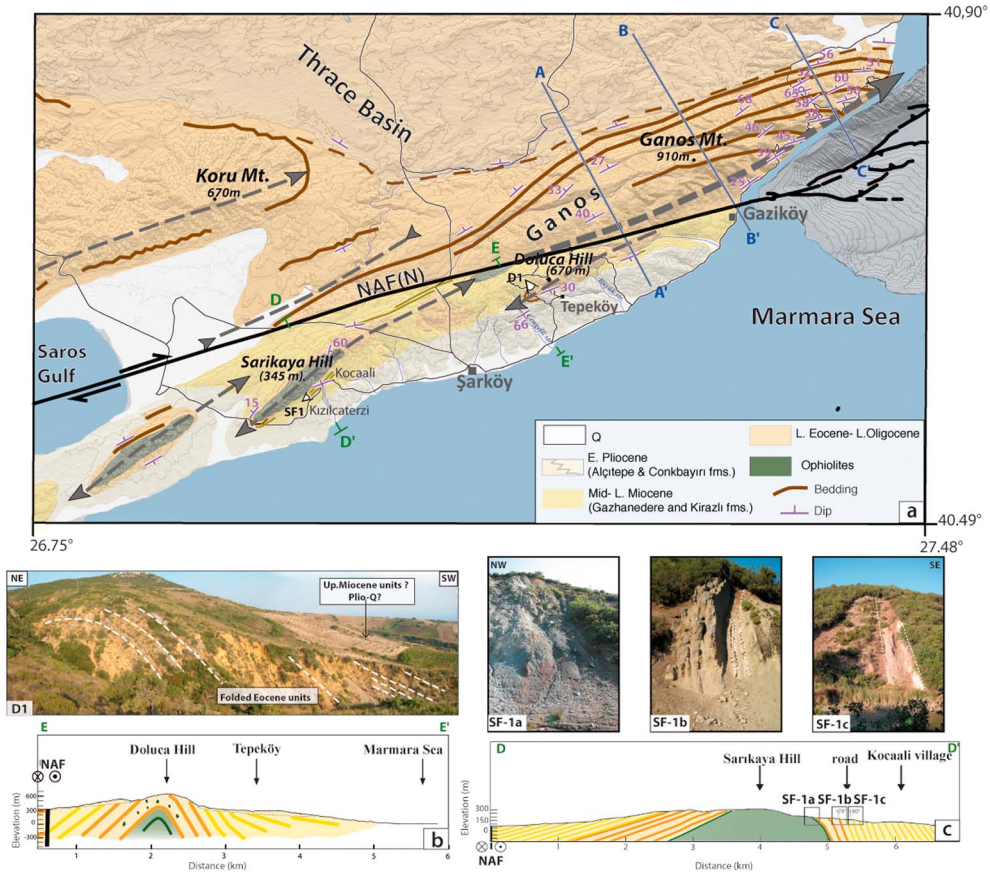

Figure 3. Northern Ganos half-anticline truncated by the NAF and associated secondary structures. (a) Geological map of southern Thrace Basin. The Ganos Anticline, north of the NAF, and secondary smaller-scale anticlines south of the NAF (from SW to NE; Tahtatepe, Sarıkaya and Doluca Folds) are obliquely cut by the north Anatolian fault. (b) Photo and cross section (D-D′) of Doluca Anticline with folded Eocene to Miocene units overlain by possibly upper Miocene sediments (see map for location). (c) Photographs and cross section (E-E′) of the Sarıkaya Anticline showing clear asymmetry with a steep southern flank.

3.2. Kilometer-Scale Folding South of the Ganos Anticline

On the northeastern part of the Gelibolu Peninsula, west of the town of Gaziköy (Figure 3a), 3-km-scale anticlines have been identified immediately south of the NAF and of the Ganos Anticline (Armijo et al., 1999, 2000). These closely spaced ~3 to 5-km-wide anticlines are structurally very similar with a narrow core of pre-Tertiary rocks consisting of olistrostomes, ophiolites, and serpentinites (attributable to the Intra-Pontide Suture; Yılmaz et al., 1997), and an envelope of Eocene-Oligocene deposits and younger Miocene rocks (Gazhanedere and Kirazlı Formations).

The northeasternmost Doluca Fold (culminating at ~670 m) is located just south of the Ganos half-anticline (Figure 3a). It is 15-km long and 3-km wide (Figures 3a and 3b). The trend of the fold axis is consistent with that of the Ganos half-anticline. The northeastern half of the Doluca Fold is truncated by the NAF. In its southwestern part, folded conformable mid-Eocene units and middle-upper Miocene units (Gazhanedere and Kirazlı Formations, respectively) dip steeply (40–50°) southeastward. No convincing field evidence of unconformable Miocene units lying on top of folded mid-Eocene units as suggested by Okay et al. (2004) were found. Therefore, folding postdates middle-upper Miocene.

The Sarıkaya Anticline has a similar shape and size to the Doluca Fold, 12-km long and 4-km wide (Figure 3a). It is however more eroded, exposing its pre-Cenozoic core and culminates at a lower elevation (~ 444 m). The Sarıkaya Fold is highly asymmetrical. Gently dipping beds are seen on its northwestern flank with an average N10°E strike. In contrast, in the steep southeastern flank, the deformed

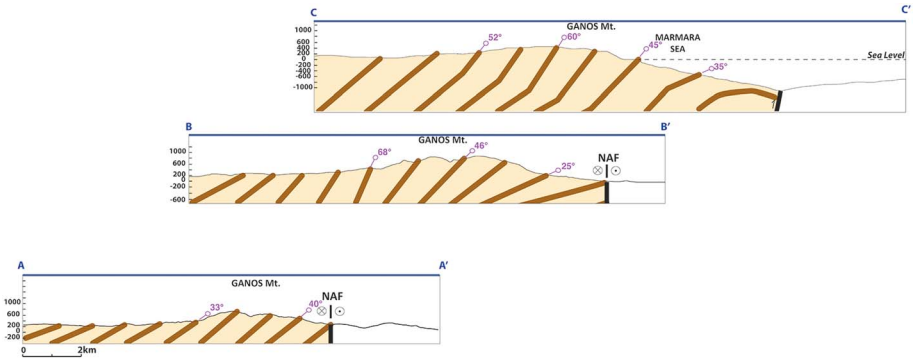

Figure 4. Structural sections across the Ganos half-anticline. Folded late Eocene-Late Oligocene units (bedding in brown) are parallel to the NAF away from the fault and become oblique and turn near the fault (A-A′, B-B′, C-C′; see Figure 3 for location). NAF = North Anatolian Fault.

Eocene-Oligocene and middle-upper Miocene rocks are subvertical (Figure 3c) with no unconformity and sit on top of the pre-Cenozoic core (Figures 3a and 3c). Therefore, as with the Doluca Anticline, folding thus occurred after the middle-upper Miocene.

The third southwesternmost anticline, Tahtatepe Fold reaches even lower elevation (~280 m). It is highly eroded and partly covered by Quaternary alluvium. Its structure is thus the least well-constrained one.

3.3. The Main Gelibolu Peninsula Fold System

Another prominent larger-scale half-anticline, similar to the Ganos Fold but more eroded, is identified farther SW on the Gelibolu Peninsula (Figures 1b, 2a, and 5). The half-anticline is 30-km long and 8-km wide with an average N45°E trend and reaches an elevation of 444 m. The Eocene-Oligocene deposits (~3.75 km thick) are folded. They consist of turbidites alternating with reef limestones and calciturbidites implying a braided fluviatile—deltaic deposition environment differing from the depositional environment in Mount Ganos (Yaltırak et al., 2000).

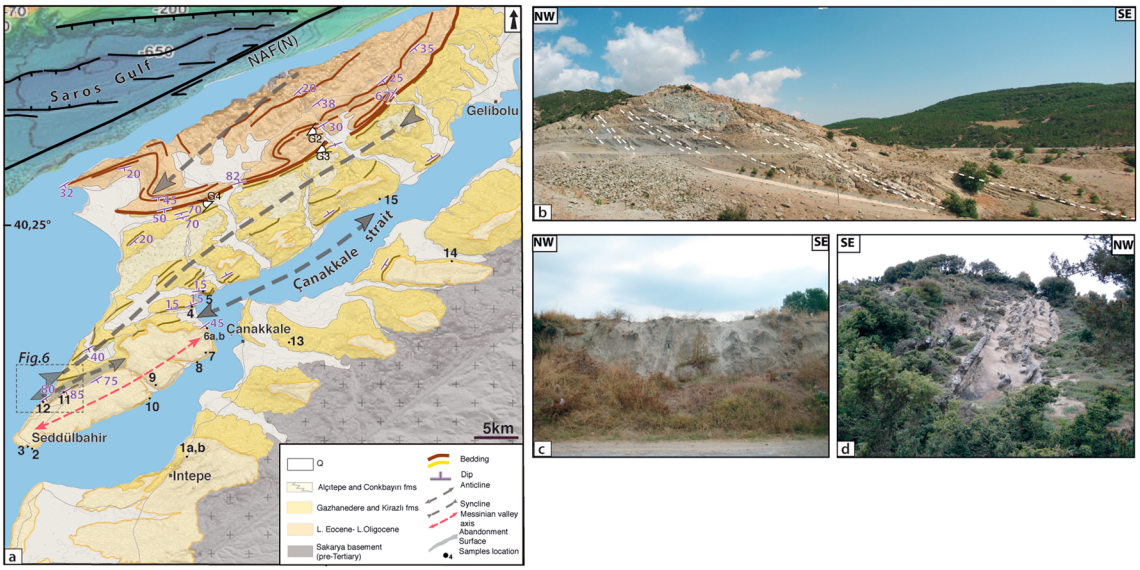

Figure 5. Southern fold system truncated by the NAF. (a) Synthetic geological map of the Gelibolu Peninsula. Folded late Eocene to earliest Pliocene units are unconformably overlain by early Pliocene (Alçıtepe Formation). Numbered sites correspond to dated biostratigraphic sections (this work and Melinte-Dobrinescu et al., 2009, see supporting information Table S1 for locations). (b) Here folded late Eocene-Late Oligocene with SE dip (site G2 on map). (c and d) Strongly folded subvertical late Miocene (Kirazlı Formation) units forming southeastern border of the Gelibolu half-anticline (sites G3 and G4). NAF = North Anatolian Fault.

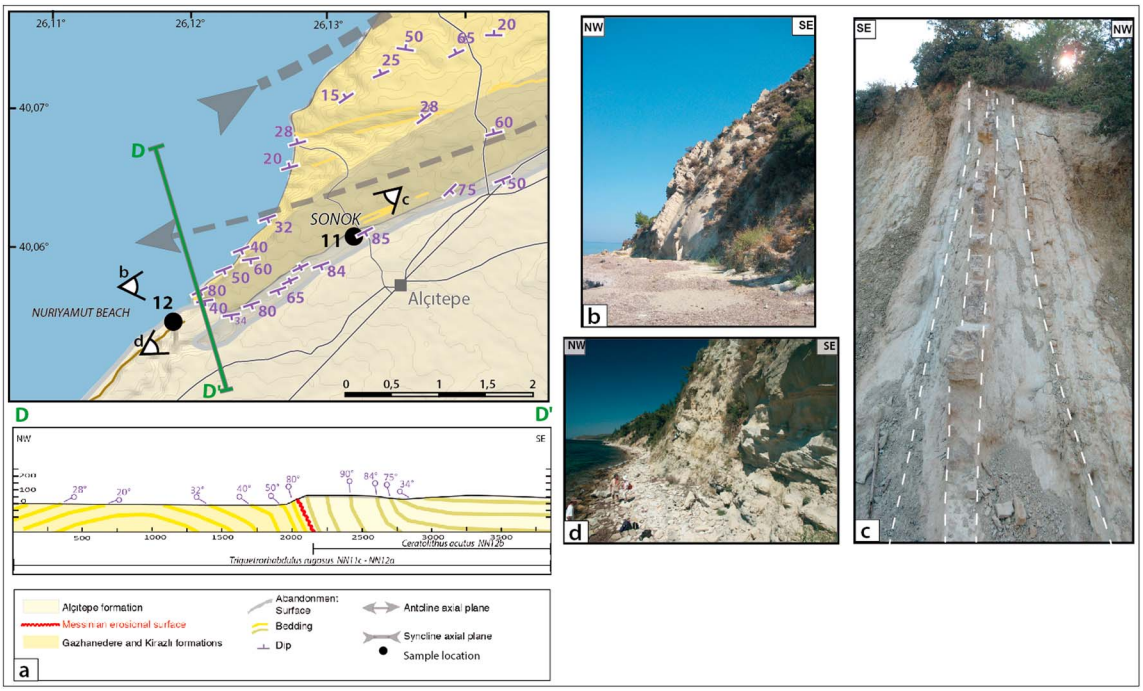

Figure 6. Detail of Gelibolu frontal anticline (see Figure 5 and Table S1 for location). (a) Top left, close-up on frontal anticline-NW border of the Messinian Valley. (bottom left, NW-SE section of flat Alçıtepe Formation (with *Ceratolithus acutus* NN12b subzone) stratigraphically overlying subvertical Alçıtepe Formation (with *C. acutus* and *Triquetrorhabdulus rugosus* NN12b subzone lower part), (d) and Kirazlı Formation (*T. rugosus* is present but not *C. acutus:* NN11c, d subzones), (b, c).

The southern end of the Thrace Basin lies on basement rocks that now outcrop in the Gelibolu Fold core. The basement is composed of Upper Cretaceous-Paleocene limestones with gentle ~15°SE dips (Figure 5a). Folded Eocene-Oligocene units become steeper and subvertical southeastward of the structure (Figures 5a and 5b). The Gelibolu half-anticline is bounded to the SE by a synclinorium of similar size. The northwestern flank of the syncline is composed of strongly folded subvertical middle-upper Miocene rocks: the continental Gazhanedere Formation and fluvio-lacustrine to marine Kirazlı Formation that we group in this study (Figures 5a, 5c, and 5d). Its southeastern end is gently dipping northwestward and overlain unconformably by late Pliocene clastic alluvial fan deposits from the Conkbayırı Formation (Önal, 1984).

On the southwestern tip of the peninsula, another small-scale anticline is identified, forming the most frontal part of the fold system (Figure 5a). That frontal anticline (Figure 6a) involves strongly folded to subvertical strata of middle-late Miocene age (Figures 6a and 6b) overlain by a unit of progressively flattening layers (Figures 6a and 6d) that form the Alçıtepe Plateau toward the SE at ~200-m elevation. This unit has been attributed to the Alçıtepe Formation with an early Pliocene age (Armijo et al., 1999), thus challenging the consensus of an older age for that formation (middle-upper Miocene, Çağatay et al., 1998; Görür & Okay, 1996; Sakınç et al., 1999; Tüysüz et al., 1998; Yaltırak, 1996).

A new and critical observation supporting an early Pliocene age for the Alçıtepe Formation as proposed by Armijo et al. (1999) is the presence of an erosional surface (highlighted in Figure 15 in Melinte-Dobrinescu et al., 2009) and of a valley incised in the folded strata of the Kirazlı Formation (late Miocene age) and parallel the present-day Dardanelles Strait (Çanakkale Strait, Figure 5a). This suggests that the Alçıtepe Formation has been deposited immediately after the marine reflooding that closed the MSC and thus overlies the subaerial Messinian erosional surface (MES). The MES is well expressed all around the Mediterranean Basin, often under the morphology of fluvial valleys (Clauzon et al., 1996). Melinte-Dobrinescu et al. (2009) confirmed the impact of the MSC in the Dardanelles region by studying 10 sites with systematic searching for calcareous nannofossils that are accurate biostratigraphic indicators. In the following section, we investigate further the impact of the MSC in seven additional critical sites (8–14 in Figures 5a and 7 and Table S1) to better constrain the tectono-stratigraphic correlation and use it as a chronometer to pinpoint the timing of compressive deformation associated to the propagation of the NAF.

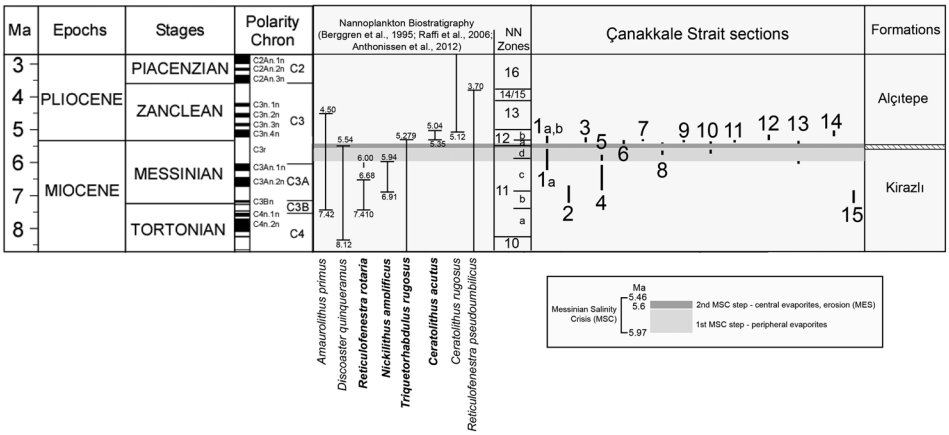

Figure 7. Chrono-biostratigraphy of the late Miocene-early Pliocene calcareous nannoplankton and inferred ages for studied sections in the Çanakkale region (Melinte-Dobrinescu et al., 2009). Chronology and calcareous nannoplankton biostratigraphy refer to Berggren et al. (1995), Raffi et al. (2006), and Anthonissen and Ogg (2012). Dark and light gray strips represent the commonly accepted two steps of the MSC (Clauzon et al., 1996). MSC = Messinian Salinity Crisis.

4. The MSC: A Robust Morphological Marker and Chronometer of Deformation

4.1. Well-Documented Large-Scale Evidence

The MSC affected the Mediterranean region in the latest Miocene as a consequence of the closure of the last gateway between the Mediterranean Sea and the Atlantic Ocean. The restricted-to-interrupted connection of the Mediterranean with the Atlantic Ocean caused a dramatic sea level drop followed by almost complete desiccation and formation of thick evaporitic deposits in the central basins and erosion and incision of deep fluvial valleys on the hinterlands and margins (Bache et al., 2015; Cita et al., 1978; Clauzon, 1973; Clauzon et al., 1996; Hsü et al., 1973).

Two successive steps have been identified with a first sea level drop of approximately 150 m between 5.97 Ma and 5.60 Ma followed by the major sea level drop of approximately 1500 m between 5.60 Ma and the end of the MSC (Bache et al., 2015; Clauzon et al., 1996, 2015; Roveri et al., 2014), proposed to be placed at 5.46 Ma (Bache et al., 2012). The MSC is also characterized by different effects that occurred during the Pliocene. The fast reflooding of the Mediterranean resulted in Gilbert-type fan deltas as sedimentary complexes filling the fluvial valleys cut during the peak of the MSC (Bache et al., 2012; Clauzon et al., 1996). Typically, these Gilbert-type fan deltas consist of two superimposed sedimentary bodies deposited over the MES (for a complete description, see Bache et al., 2012, Figure 2). The underlying and mainly distal body builds up in a subaquatic environment and is formed by sandy to conglomeratic foreset and clayey bottomset beds while the overlying and mainly proximal body is a subaerial alluvial fan forming sandy to conglomeratic topset beds. Their topmost part is marked by an abandonment surface. Such paleogeographical entities have been identified on this basis and dated by calcareous nannofossils in the Dardanelles by Melinte-Dobrinescu et al. (2009) and Suc et al. (2015).

The identified fluvial valley, which we call the Messinian Valley, has been characterized by Melinte-Dobrinescu et al. (2009, Figure 15) not only stratigraphically in a cross section but also cartographically beneath the Gelibolu Peninsula. At the tip of the peninsula, the northern and southern flanks of the Messinian Valley drafted in Figure 9c can clearly be observed at Nuriyamut Beach and Seddülbahir, respectively.

4.2. Impact of the MSC in the Dardanelles: Stratigraphic and Tectonic Correlation

In their stratigraphic review, Melinte-Dobrinescu et al. (2009) examined 12 key sections. Here we focus on eight of them (1–7 and 15) plus seven additional localities (8–14) (Figure 5a and Table S1) sampled in the Kirazlı and Alçıtepe Formations in the Dardanelles and dated by the calcareous nannofossils that they contain (Figure 7). This figure shows the well-known distribution, in a relatively short time interval, of eight calcareous nannofossil species, the First Appearance Datum (FAD) and/or Last Appearance Datum (LAD) of six of them

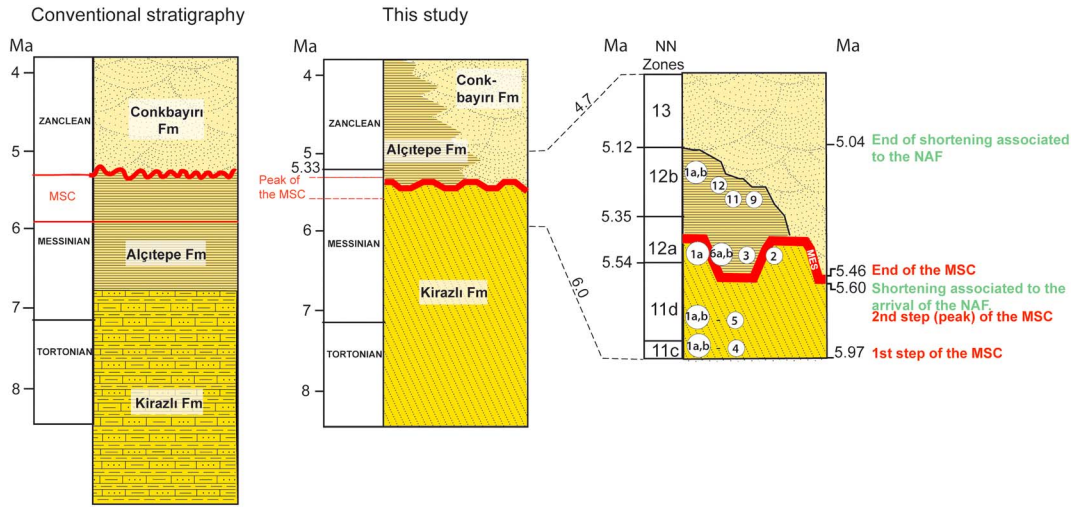

Figure 8. Controversial stratigraphy of the late Miocene-early Pliocene in the Canakkale region. Conventional stratigraphy (e.g., Görür et al., 1997; Sakınç et al., 1999; Yaltırak et al., 2000; Türkecan & Yurtsever, 2002; Çağatay et al., 2006) suggests gradual transition from the Kirazlı to the Alcıtepe Formations (Messinian age in this case) capped by the Zanclean Conkbayırı Formation. In this study (middle) angular and erosional (MES) unconformities between the Alçıtepe and Kirazlı Formations supported by calcareous nannoplankton biostratigraphy (Figure 7) explain well the stratigraphic setting. To the right: Detail corresponding to the top of the Kirazlı Formation and base of the Alçıtepe Formation at sites such as Sonok and Nuriyamut Beach (see Figure 5), with location of dated sections. MES = Messinian erosional surface; NAF = North Anatolian Fault; MSC = Messinian Salinity Crisis.

were used: *Amaurolithus primus* (FAD: 7.42 Ma; LAD: 4.50 Ma), *Reticulofenestra rotaria* (FAD: circa 7.41 Ma; LAD: inaccurate, up to 6 Ma), *Nickilithus* (= *Amaurolithus*) *amplificus* (FAD: 6.91 Ma; LAD: 5.94 Ma), *Triquetrorhabdulus* (= *Orthorabdus*) *rugosus* (FAD: 12.67 Ma; LAD: 5.20 Ma), *Ceratolithus acutus* (= *C. armatus*) (FAD: 5.35 Ma; LAD: 5.04 Ma), *Ceratolithus rugosus* (FAD: 5.12 Ma), and *Reticulofenestra pseudombilicus* (FAD: 8.76 Ma; LAD: 3.70 Ma).

Taking into account the chronology of the MSC, to distinguish the deposits overlying the MES from those impacted by the fluvial erosion, that is, how to reorganize the Gazhanedere, Kirazlı, and Alçıtepe Formations with respect to this morphology, refers to the occurrence of the species *C. acutus* with or without *T. rugosus* (NN12a and 12b subzones, respectively), in the absence of *Discoaster quinqueramus* not recorded in the Dardanelles area. The main outcome of Melinte-Dobrinescu et al. (2009) extensive investigation is that the Alçıtepe Formation was deposited just after the fast marine reflooding that ended the MSC at 5.46 Ma in the latest Messinian (Bache et al., 2012).

In their most complete section 1a,b (Figures 5a, 7, and 8), Melinte-Dobrinescu et al. 2009 find evidence for embayment marine conditions with a sedimentary hiatus marked by oxidized claystones overlying a coastal lignite containing *T. rugosus* and overlain by clays containing this species plus *C. acutus* (for detailed interpretation, see Melinte-Dobrinescu et al., 2009). It has been demonstrated that, laterally, this sedimentary gap corresponds to the MES, here overlain by foreset beds of a Gilbert-type fan delta. The bottomset beds of this Gilbert-type fan delta are exposed in the West Seddülbahir section 3, which first displays *T. rugosus* and then this species with *C. acutus* (NN 12a, 12b subzones; Melinte-Dobrinescu et al., 2009). The sections sampled in the Kirazlı Formation that deposited prior to the MES (sections 2, 4, 5, 6b, and 15; Figure 7) have *T. rugosus* among other calcareous nannofossils but lack systematically in *C. acutus* (see Melinte-Dobrinescu et al., 2009 for details). This implies a latest Tortonian to early Messinian age (NN11 zone).

The systematic presence of the discriminant *C. acutus*, the importance of which has been recently emphasized (Popescu et al., 2017), in the bottomset beds of the Gilbert-type fan deltas above the identified MES (Figures 6a, 7, and 8; sections 1a, b, 3, 6a, 7) places definitively the Alçıtepe Formation within the early Zanclean. The seven additional sections (see above; Figures 5a and 7) support the above analysis.

The southern border of the Messinian Valley (Figure 5a) is marked by gently NW dipping sandstones of the Kirazlı Formation cut by the MES and overlain by flattening limestones of the Alçıtepe Formation (Figure 5;

Melinte-Dobrinescu et al., 2009, Figure 15). Section 8 (Karıntepe), 15 m above the sea level, shows the gently dipping marine sediments of the Kirazlı Formation that provided one discriminating calcareous nannofossil, *T. rugosus*, cut by the MES. Here *C. acutus* is absent from the Gilbert-type fan delta that overlies the Kirazlı Formation at an angular unconformity corresponding to the MES. This section hence spans from NN11a or NN11d subzones (Tortonian or late Messinian) to NN12a subzone (latest Messinian) (Figures 7 and 8). Section 9 (Melekhanım), 55 m above sea level, exhibits a Gilbert-type delta and provides two discriminating calcareous nannofossils, *T. rugosus* and *C. acutus*. This section is post-MSC and ascribed to the lower part of the NN12b subzone (latest Messinian to earliest Zanclean). Section 10 (Karanfil T.), collected at sea level, involves the Kirazlı and Alçıtepe Formations separated by the MES. *T. rugosus* is present in the three samples collected above the MES, and *C. acutus* occurs in the uppermost one, about 3 m above the MES. Here the Alçıtepe sediments belong to the NN12a subzone lower part-NN12b subzone lower part (Figures 7 and 8). This section thus clearly shows deposits from pre-MSC (Tortonian-Messinian) to post-MSC (latest Messinian–earliest Zanclean).

The northern border of the Messinian Valley at the tip of the Gelibolu Peninsula (section 3.3) is the most critical locality where distinction of the two formations is possible. On the Nuriyamut Beach, subvertical layers previously identified as belonging to the Kirazlı Formation by Armijo et al. (1999) are separated by less than 250 m from gently folded to nearly flat layers that are part of the Alçıtepe Formation (Figures 6a, 6b, and 6d). Samples from section 12 (Nuriyamut Beach) and 11 (Sonok) are 500 m apart from each other. They are located west of the Alçıtepe village and at the historical site of Sonok, respectively (see Figures 6a and 6c). Section 11, sampled 80 m above sea level, contains *T. rugosus* in addition to *C. acutus*, which constrains the underlying part of section 12 in the early 12b NN subzone (latest Messinian to earliest Zanclean). Section 12 collected along the seashore in folded sediments that we ascribe now to the Alçıtepe Formation contains *C. acutus* alone (i.e., without *T. rugosus*) in its upper part. This places its deposition in late NN 12b subzone (earliest Zanclean). The systematic use of calcareous nannoplankton allows reassessment of debated regional stratigraphic, lithological, and tectonic correlations in the Dardanelles (Çanakkale region) (Figure 8). We use these data to capture the timing of compressive deformation at the tip of the propagating NNAF.

5. Discussion

5.1. Reconstruction of Initial Fold Geometry in the Dardanelles

Aside from a few schematic sections by Yaltırak (1996), no satisfying structural section has shown so far the link between the fold system underlying Mount Ganos, the Gelibolu Peninsula fold system, and the NNAF. Our composite section is of crustal scale and restores the Ganos-Gelibolu Fold along the ~70 km visible (on land) trace of the NNAF prior the offset (Figures 1b and 2). The geometry of reconstructed structures is consistent with field observations (Figure 9a, see Figure 2 for location) while not being unique. The inferred south verging asymmetrical fold geometry differs from the flat negative flower structure flanked by a constraining bend model responsible for the uplift of Mount Ganos, as suggested by Okay et al. (1999). It does not support either the crustal-scale ramp monocline geometry of Mount Ganos above a northward dipping NAF (Ganos Fault) deforming at least since the last 2 Ma as proposed by Okay et al. (2004).

Differences in thickness and depositional environment of Eocene-Oligocene units across the NNAF may be explained by the preexisting configuration of the Thrace Basin. The Thrace Basin is considered to have formed in mid-Eocene after the collision between the Sakarya continent and the Rhodope-Pontide massif (Turgut et al., 1991; Tüysüz et al., 1998). The southern end of the Thrace Basin lies on top of the IPSZ, with traces identified south of the NAF and on the Gelibolu Peninsula (Figure 1b) (Şentürk & Okay, 1984; Şengör & Yılmaz, 1981; Yılmaz & Clift, 1990; Görür & Okay, 1996). The only published basin-scale section is focused on the northern, deepest part of the Thrace Basin, north of the NAF (Görür & Okay, 1996). We propose that the southern end of the Thrace Basin occurs south of the NAF within the Dardanelles and has a southward tapered basin edge shape (Figures 9a, 9c, and 10). Therefore, the thickness of the Eocene-Oligocene sequence observed in Mount Ganos (~5.5 km) is greater than the thickness on the Gelibolu Peninsula for the equivalent sequence (~3.75 km). Mount Ganos half-anticline is higher (924 m) than the Gelibolu half-anticline (444 m). The latter dies out by right-lateral offset, after the NAF fully propagates (vertically and horizontally) and becomes a passive marker (Figure 10, left). Although

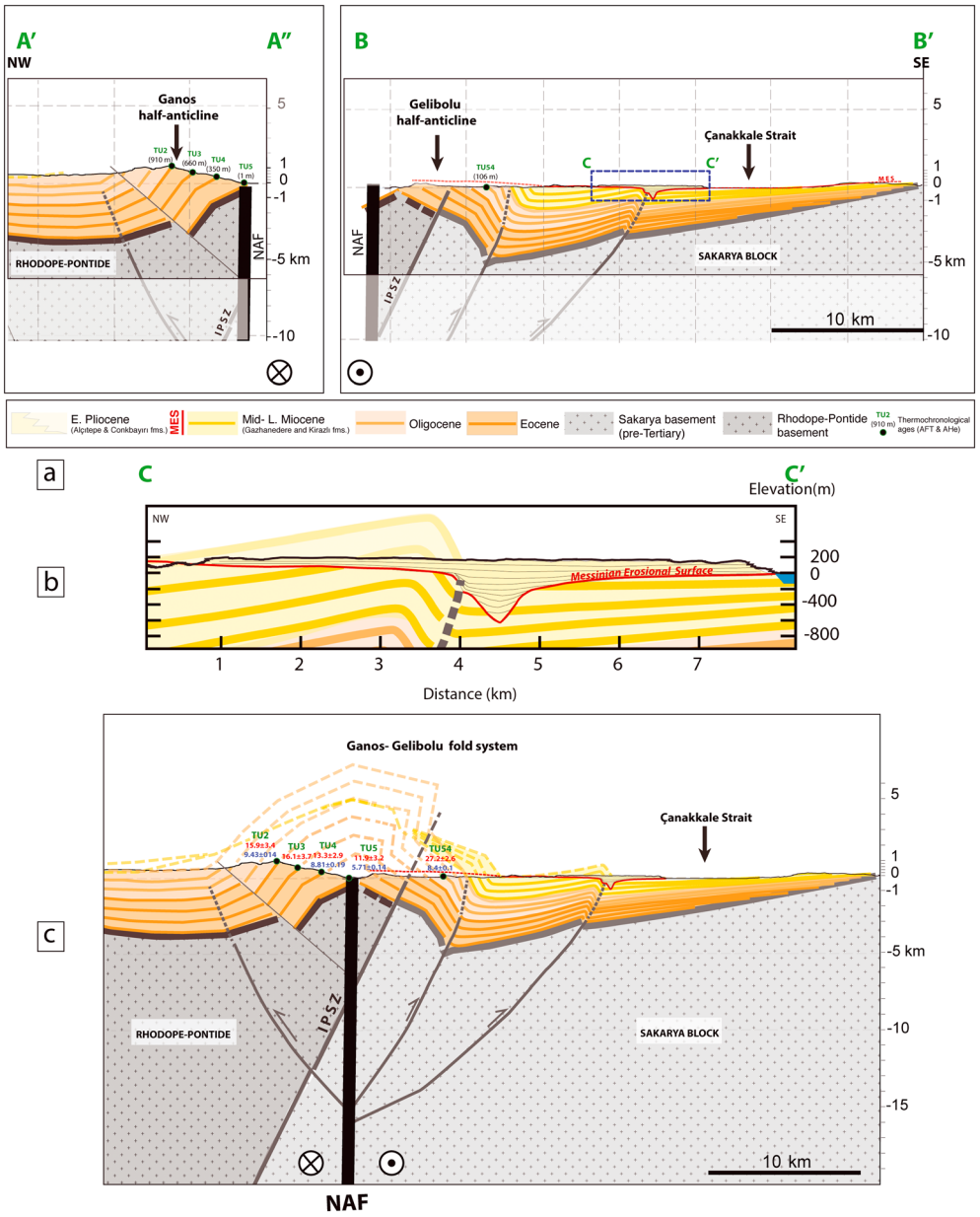

Figure 9. Composite NW-SE cross section of the Ganos-Gelibolu fold system and detail of the frontal fold. (a) The Ganos half-anticline involves pre-Tertiary basement (Rhodope-Pontide) and late Eocene to late Oligocene sedimentary rocks. The basement does not outcrop on this side of the NAF (top right). The Gelibolu fold system involves pre-Tertiary basement (Sakarya Block), late Eocene to earliest Pliocene rocks. Cretaceous limestones outcrop on the northwestern part of the Gelibolu Peninsula (see Figure 5). (a and c) Undoing the 70 km right-lateral offset and 5° clockwise rotation of the Gelibolu "Block" restores the complete geometry of the anticline while matching the Ganos and Gelibolu half-anticlines. The folded southern end of the Thrace Basin is lying unconformably on the junction of two basements: The Rhodope-Pontide basement to the north and the Sakarya Block to the south**.** This junction is a suture zone known as "Intra-Pontide Suture Zone" (IPSZ). The North Anatolian Fault tip butts against the IPSZ and reactivates the preexisting oblique structure. Thermochronology results from Zattin et al. (2005, 2010) are indicated (apatite fission track ages in red and apatite (U-Th)/He ages in blue). Main folding of the Thrace Basin southern end forming the Ganos-Gelibolu Fold system then occurs above a compressive flower structure that is afterward sheared and offset by the NAF (b). The frontal anticline is characterized by NW gently dipping layers and a steep-subvertical-southeastern border where the Messinian Valley is carved. The northwestern border of the valley as well as part of the filling are also affected by folding. The end of the folding is clearly evidenced by an unconformity between the early Pliocene (Zanclean) flat marine sediments and the earliest Pliocene (early Zanclean) vertical marine sediments. NAF = North Anatolian Fault.

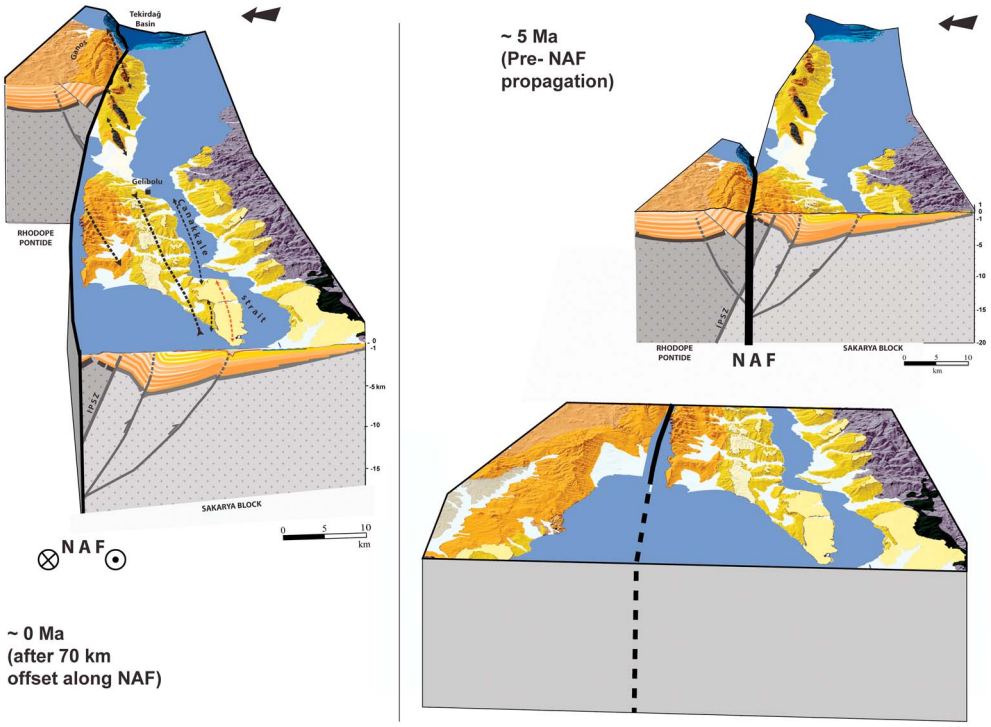

Figure 10. Three-dimensional sketches of the Ganos-Gelibolu fold system. (right) Restored state at ~5 Ma just before NAF propagation across the folded structure. The folded southern end of the Thrace Basin is lying unconformably on the two basements bounded by the IPSZ (Saner, 1980). Southwestward propagation of the NAF reactivates the oblique IPSZ and produces folding for ~0.56 Myr and while the Mediterranean and the Aegean were affected by the MSC. Compressive deformation basically stops when the NAF eventually reaches the surface, in early Pliocene, and starts propagating southwestward causing progressively a 70-km right-lateral offset of the Ganos-Gelibolu Folds (final state illustrated to the left). Note the transition of the Gelibolu half-anticline from an active marker of shortening giving way to secondary smaller-scale folds that emerge locally and successively while the NAF propagates. NAF = North Anatolian Fault; MSC = Messinian Salinity Crisis; IPSZ = Intra-Pontide Suture Zone.

considerably reduced, the remaining uplift occurs not only on Mount Ganos side as implied in Seeber et al. (2004) but also on both sides of the restraining bend.

The kilometric-scale fold system supported by the basal basin units and basement outcrop indicates a crustal depth for the present restraining bend of the NNAF (~15–20 km). To explain the geometry of the Ganos-Gelibolu fold system, we propose a flower structure with three splays (Figures 9c and 10, right): two northwestward dipping thrusts responsible for the southeastward propagation of folding by steepening of the main (Ganos-Gelibolu) and frontal anticlines southern flanks; a third thrust dipping southeastward responsible for the uplift of the northern part of the main anticline exhuming basal Eocene sediments in Mount Ganos.

5.2. Timing and Rate of Folding

The morphostructural description of the features in the Dardanelles Strait region and the presence of marine sediments deposited in Gilbert-type fan deltas make their correlation possible with the interplay between NAF-related tectonic deformation and the large sea level changes in the Mediterranean Basin associated with the MSC.

The unconformity between the folded upper Miocene-lower Pliocene (subvertical Kirazlı and Alçıtepe Formation layers observed on the Nuriyamut Beach and at Sonok, respectively) and the flat nearly undeformed early Pliocene units (Alçıtepe Formation, observed at Seddülbahir and Intepe among other sites, see Figure 5 for location) first discussed by Armijo et al. (1999) is supported now by our morphostructural characterization of the frontal deformation (Figure 6). The earliest Zanclean marine deposits were affected by folding of the frontal anticline while they were filling the Messinian Valley. This inference is consistent

with the late Messinian age proposed for the deformation of the Dardanelles (Çanakkale region) by Armijo et al. (1999). Previously attributed ages to the Alçıtepe Formation were based on inaccurate lithological correlations (Sakınç et al., 1999). The Alçıtepe Formation is composed of alternating sandstones and limestones similar to the Kirazlı Formation (Figures 6b and 6d) and with brackish Paratethyan fauna (Sümengen & Terlemez, 1991). This type of assemblage is generally assigned to Paratethyan origin (of which the Black Sea is a residual basin) with middle-upper Miocene age (Pontian Paratethyan Stage) with intercalations of layers that contain Mediterranean marine fauna (Ostrea and Pecten). The presence of these mollusk macrofossils may be taken as evidence of marine transgression that connected the Black Sea and the Aegean Sea/Mediterranean Sea through the Sea of Marmara during middle-upper Miocene (Çağatay et al., 2006). However, as they may have a large range of salinity tolerance and duration (Sakınç et al., 1999) they are not discriminant markers for the impact of the MSC and cannot be used for precise dating of folding and paleo-environmental change.

The distribution in time of two discriminating calcareous nannofossils *T. rugosus* and *C. acutus* present in reference sections (Figures 6 and 7, Sites 2–3; Site 1a,b; Site 11, and Site 12) convincingly solves the confusion due to the lithological similarities (Sakınç et al., 1999; Yaltırak et al., 2000). The above inferences remove any remaining doubt about the stratigraphic and structural position of both the Kirazlı and Alçıtepe Formations. The previous arguments of (1) conformable Kirazlı and Alçıtepe Formations marked by gradational variations and (2) an unconformity between the Conkbayırı Formation and the above-cited formations (Yaltırak et al., 2000) ignore the impact of the MSC in the Dardanelles. We conclude that only morphological and reliable biostratigraphic markers allow proper correlation of the stratigraphic units in question (Figure 8). Folding prior to right-lateral offset by the NAF started in the late Messinian (Kirazlı Formation: NN11d subzone upper part, at about 5.60 Ma) affecting Eocene-Oligocene, Miocene to earliest Pliocene sediments (as seen on the northern border of the Messinian Valley, Figures 6 and 9, bottom). It stopped in the early Zanclean (Alçıtepe Formation: NN12b subzone upper part, at about 5.04 Ma) resulting in approximately 0.56 Myr of shortening.

The total horizontal shortening across the Ganos-Gelibolu fold system measured on our composite section by restoring the layer at the base of Gazhanedere-Kirazlı Formations (see Figure 9a) is ~ 5.7 ± 0.2 km. This amount corresponds to a maximum of shortening absorbed by this layer and unit as interpreted in our section. The minimum total horizontal shortening measured by restoring the topmost layer of the Gazhanedere-Kirazlı Formations (of Messinian age) is ~3.1 ± 0.2 km. The deduced shortening rate ranges between ~0.55 ± 0.3 and 1.2 ± 0.3 cm/year over ~0.56 Myr with a corresponding horizontal slip range ~0.275–0.5 cm/year after projection on the NNAF. These rapid rates can be explained by and associated with nascent plate boundary processes.

The link between the Thrace Basin tectonic deposition environment (extension and convergence) and the IPZS is yet to be understood. Recently, low-temperature thermochronological studies carried out on a section on Mount Ganos, by Zattin et al. (2005, 2010), have suggested late Oligocene and middle Miocene exhumation events. These results (see Figure 9 for sample location and apatite fission track and (U-Th)/He ages) support the fact that the sampled section of Mount Ganos and Gelibolu was already brought at relatively shallow depth by folding in late Miocene (see TU5, AHe ages in blue in Figure 9c; Zattin et al., 2010). The blind reverse faults on both sides of the NAF in Figure 9c would be responsible for the pre-NAF relief formation and then would be taken over by the flower structure forming at the extremity of the fault (NAF). It is thus likely that the estimated shortening range above accounts for two episodes of deformation: one in late Oligocene-middle Miocene and one in late Miocene-early Pliocene in agreement with low-temperature thermochronology (Zattin et al., 2005, 2010). In order to distinguish between the two deformation stages, inherited structures from earlier tectonic episodes have to be better determined and quantified.

Full vertical and horizontal propagation of the NNAF is followed by displacement along the fault giving way to an offset of the Ganos-Gelibolu folds with an average slip rate of 14 mm/year (70 km southwestward offset over the last 5 Myrs). Adding the SNAF gives an average total slip rate of 17 mm/year between Eurasia and Anatolia with a total offset across the Marmara region of 85 km (Armijo et al., 1999). The estimated geological slip rates are lower than the 25 ± 2 mm/year GPS slip rates around Marmara (Ergintav et al., 2014). This change of rate in time can be explained by a change in plate boundary conditions induced by NAF growth.

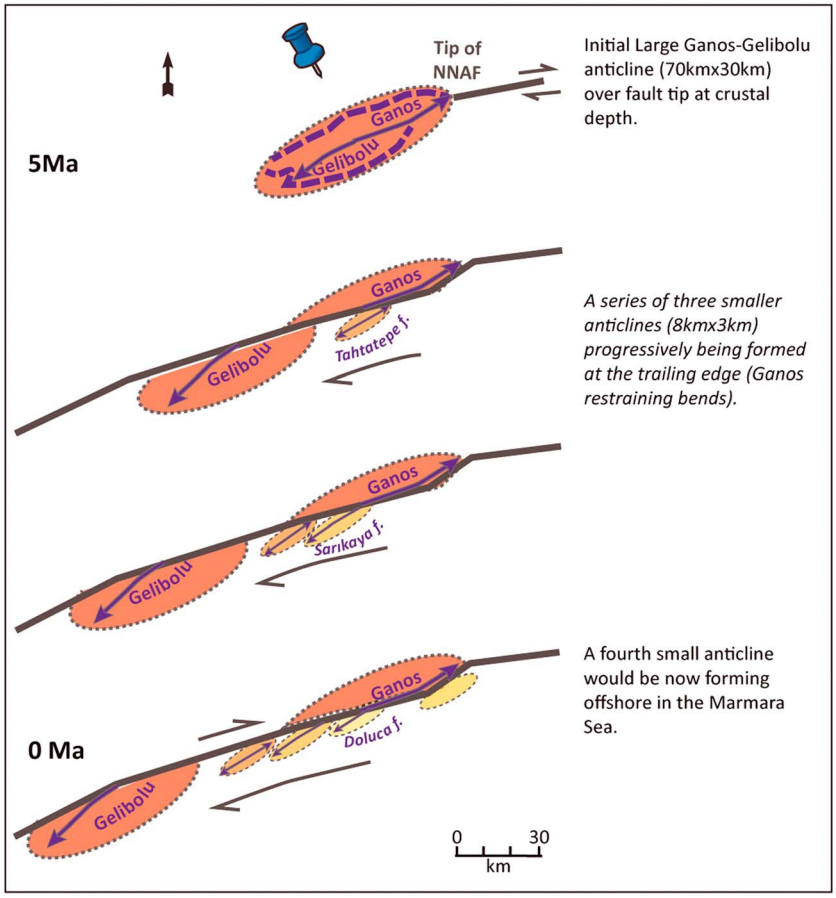

Figure 11. Evolution of folding in the Dardanelles (in the last 5 Ma). From top to bottom: The initial large Ganos-Gelibolu Anticline (shown in reddish tone) forms at the tip of the NNAF prior to its vertical and horizontal propagation. After full vertical propagation of the fault, the progressive accumulation of right-lateral displacement on the NAF deactivates the southern half of the initial large fold. A series of smaller anticlines (shown in orange and yellow tones) continue to progressively form on top of the Ganos kink or restraining bend. The decrease of present-day elevation and the increase of the degree of erosion and degradation of the folded structure from the NE (Doluca Anticline) to the SW (Tahtatepe Anticline) suggest a similar NE-SW trend in the age of folding with the Doluca Fold being the youngest of those three anticlines. A fourth one would be now forming at the Ganos kink offshore in the Marmara Sea. NAF = North Anatolian Fault; NNAF = north NAF.

5.3. Continued Folding After NAF Propagation

Our study shows that the Messinian-Zanclean stage of folding is associated to propagation processes at the tip of the fault, in other terms to compressional deformation at the tip of the nascent plate boundary. Only after full vertical and then lateral propagation, the NAF geometry is imposed and deformation associated to the newly acquired geometry can occur. Only after this stage, slip on the fault can take place and is partitioned depending on the imposed geometry. Continuing right-lateral displacement on the NAF has progressively produced younger folds above the long-lived compressive fault bend (Tahtatepe, Sarıkaya, and Doluca folds, respectively; Figures 3 and 11). North of the NAF and of the restraining bend, the Mount Ganos Anticline continues to grow and is still considered as an active marker of deformation as opposed to the Gelibolu Anticline that becomes a passive marker (Figure 11). The trailing edge secondary folds formed on top of the Ganos bends/kink are comparable features in terms of tectonic setting and geometry to transpressional folds in analog models (Cooke et al., 2013; McClay & Bonora, 2001) and described at other plate boundaries such as the San Andreas Fault (e.g., Bürgmann, 1991; Titus et al., 2007). The finite deformation observed in the Marmara Sea is strictly associated to postpropagation partitioned slip on the NAF and therefore described as a releasing bend/step-over or pull-apart basin (Armijo et al., 2002).

6. Conclusions

The Ganos-Gelibolu fold system is a kilometric-scale morphostructural marker of propagation processes of a nascent right-lateral continental plate boundary (Armijo et al., 1999). The analysis of the interplay between deformation and outstanding sea level changes in the Mediterranean allows us to trace back in time the evolution of the southern Thrace Basin margin (Melinte-Dobrinescu et al., 2009) in response to localization and propagation of the NAF. Our detailed mapping and structural analysis allow us to define the Ganos-Gelibolu Fold as an oblique asymmetrical anticline flanked by a syncline-frontal anticline system in its southeastern part. The Dardanelles fold system formed as an expression of intense and rapid compressive deformation of the Dardanelles (Çanakkale region) in response to the fault localization and propagation. Also, we explain the formation of transpressional secondary smaller-scale folds south of the NAF and in front of Mount Ganos by a bypassed hence less active fault bend.

Biostratigraphic analysis combined with morphostructural analysis in the Dardanelles clarify the debate on regional stratigraphy and allows to pinpoint the timing of deformation with a high-resolution correlation. Compressive deformation at the propagating tip of the NAF started during the MSC and involved middle Eocene to late Miocene (late Messinian)-earliest Pliocene (early Zanclean) units. Deformation end is marked by an angular unconformity between strongly to gently folded late Messinian-earliest Zanclean marine units (~5.60 Ma) and intact early Zanclean trangressive marine units (~5.04 Ma). Rapid crustal shortening of several kilometers across the Ganos-Gelibolu fold system ends when the NAF reaches the surface while propagating and coincides with the marine reflooding of the region.

At a larger scale, characterization of such crustal deformation in the Dardanelles and the Marmara Sea (over a hundred kilometers of distance) is a key and unique element to constrain NAF fault tip behavior before entering the Aegean extensional domain where collision-driven extrusion along lithospheric faults reactivates and propagates through preexisting structures.

Acknowledgments

This work was supported by a PhD grant to Ç. Karakaş by the French Ministry of Education, and funded by ANR project EGEO (ANR-06-BLAN-0156 CSD 6). We thank Bertrand Meyer and Gwénael Jouannic (Pierre et Marie Curie University), Ziyadin Çakır and Gülsen Uçarkuş (Istanbul Technical University, İTÜ), and Laureen Drab for their help and support in the field. Our late colleague Georges Clauzon took part in field investigations. The authors thank Sarah Titus and Christopher C. Sorlien for their constructive reviews as well as the Associate Editor her/his comments. The biostratigraphic data (list of microfossils, interpretation in terms of nannozones and deduced ages) are accessible from https://figshare.com/s/5b3c53307e3da6788b1d.The other data that support the findings of this study are available within the publication (structural cartography) or in referenced studies. This is IPGP contribution 3935.

References

Akbayram, K., Sorlien, C. C., & Okay, A. I. (2016). Evidence for a minimum 52±1 km of total offset along the northern branch of the North Anatolian Fault in northwest Turkey. *Tectonophysics*, *668*, 35–41.

Anthonissen, D. E., & Ogg, J. (2012). Cenozoic and cretaceous biochronology of planktonic foraminifera and calcareous nannofossils. In F. Gradstein, et al. (Eds.), *The geological time scale 2012* (Vol. 3, pp. 1083–1127). Amsterdam, Netherlands: Elsevier, Appendix.

Armijo, R., Flérit, F., King, G., & Meyer, B. (2003). Linear elastic fracture mechanics explains the past and present evolution of the Aegean. *Earth and Planetary Science Letters*, *217*(1), 85–95.

Armijo, R., Meyer, B., Hubert, A., & Barka, A. (1999). Westward propagation of the North Anatolian Fault into the northern Aegean: Timing and kinematics. *Geology*, *27*(3), 267–270.

Armijo, R., Meyer, B., Hubert, A., & Barka, A. (2000). Westward propagation of North Anatolian Fault into the northern Aegean: Timing and kinematics: Comment and reply. *Geology*, *28*(2), 188–189.

Armijo, R., Meyer, B., King, G. C. P., Rigo, R., & Papanastassiou, D. (1996). Quaternary evolution of the Corinth rift and its implications for the Late Cenozoic evolution of the Aegean. *Geophysical Journal International*, *126*(1), 11–53.

Armijo, R., Meyer, B., Navarro, S., King, G. C. P., & Barka, A. (2002). Asymmetric slip partitioning in the Sea of Marmara pull-apart: A clue to propagation processes of the North Anatolian Fault? *Terra Nova*, *14*(2), 80–86.

Armijo, R., Pondard, N., Meyer, B., Uçarkus, G., Mercier De Lépinay, B., Malavieille, J., et al. (2005). Submarine fault scarps in the Sea of Marmara pull-apart (North Anatolian Fault): Implications for seismic hazard in Istanbul. *Geochemistry, Geophysics, Geosystems*, *6*, Q06009. https://doi.org/10.1029/2004GC000896

Bache, F., Gargani, J., Suc, J.-P., Gorini, C., Rabineau, M., Popescu, S.-M., et al. (2015). Messinian evaporite deposition during sea level rise in the Gulf of Lions (western Mediterranean). *Marine and Petroleum Geology*, *66*, 262–277.

Bache, F., Popescu, S.-M., Rabineau, M., Gorini, C., Suc, J.-P., Clauzon, G., et al. (2012). A two-step process for the reflooding of the Mediterranean after the Messinian Salinity Crisis. *Basin Research*, *24*, 125–153.

Barka, A. A. (1992). The North Anatolian Fault zone. *Annales Tectonicae*, *6*, 164–195.

Bécel, A., Laigle, M., de Voogd, B., Hirn, A., Taymaz, T., Galvé, A., et al. (2009). Moho, crustal architecture and deep deformation under the north Marmara trough, from the SEISMARMARA Leg 1 offshore–onshore reflection–refraction survey. *Tectonophysics*, *467*(1), 1–21.

Bécel, A., Laigle, M., De Voogd, B., Hirn, A., Taymaz, T., Yolsal-Cevikbilen, S., & Shimamura, H. (2010). North Marmara trough architecture of basin infill, basement and faults, from PSDM reflection and OBS refraction seismics. *Tectonophysics*, *490*(1), 1–14.

Berggren, W. A., Kent, D. V., Swisher, C. C. III, & Aubry, M.-P. (1995). A revised Cenozoic geochronology and chronostratigraphy. In W. A. Berggren, et al. (Eds.), *"Geochronology Time Scales and Global Stratigraphic Correlations", SEPM (Society for Sedimentary Geology), Special Publication* (Vol. 54, pp. 141–212).

Bilham, R., & King, G. (1989). The morphology of strike-slip faults: Examples from the San Andreas fault, California. *Journal of Geophysical Research*, *94*(B8), 10,204–10,216.

Bürgmann, R. (1991). Transpression along the Southern San Andreas Fault, Durmid Hill, California. *Tectonics*, *10*(6), 1152–1163. https://doi.org/10.1029/91TC01443

Çağatay, M. N., Görür, N., Flecker, R., Sakınç, M., Tünoğlu, C., Ellam, R., et al. (2006). Paratethyan–Mediterranean connectivity in the Sea of Marmara region (NW Turkey) during the Messinian. *Sedimentary Geology*, *188*, 171–187.

Çağatay, N., Görür, N., Alpar, B., Saatçılar, R., Akkök, R., Sakınç,, M., et al. (1998). Geological evolution of the Gulf of Saros, NE Aegean Sea. *Geo-Marine Letters*, *18*, 1–9.

Carton, H., Singh, S. C., Hirn, A., Bazin, S., De Voogd, B., Vigner, A., et al. (2007). Seismic imaging of the three-dimensional architecture of the Çınarcık Basin along the North Anatolian Fault. *Journal of Geophysical Research*, *112*, B06101. https://doi.org/10.1029/2006JB004548

CIESM (2008). Executive summary. In F. Briand (Ed.), *The Messinian Salinity Crisis from mega-deposits to microbiology – A consensus report*, *CIESM Workshop Monographs* (Vol. 3, pp. 7–28). Monaco: CIESM.

Cita, M. B., Ryan, W. B. F., & Kidd, R. B. (1978). Sedimentation rates in Neogene deep sea sediments from the Mediterranean and geodynamic implications of their changes. *Initial Reports of the Deep Sea Drilling Project*, *42A*, 991–1002.

Clauzon, G. (1973). The eustatic hypothesis and the pre-Pliocene cutting of the Rhône Valley. *Initial Reports of the Deep Sea Drilling Project*, *13*(2), 1251–1256.

Clauzon, G., Suc, J.-P., Do Couto, D., Jouannic, G., Melinte-Dobrinescu, M. C., Jolivet, L., et al. (2015). New insights on the Sorbas Basin (SE Spain): The onshore reference of the Messinian Salinity Crisis. *Marine and Petroleum Geology*, *66*, 71–100.

Clauzon, G., Suc, J.-P., Gautier, F., Berger, A., & Loutre, M. F. (1996). Alternate interpretation of the Messinian Salinity Crisis: Controversy resolved? *Geology*, *24*(4), 363–366.

Cooke, M. L., Schottenfeld, M. T., & Buchanan, S. W. (2013). Evolution of fault efficiency at restraining bends within wet kaolin analog experiments. *Journal of Structural Geology*, *51*, 180–192.

Ergintav, S., Reilinger, R. E., Çakmak, R., Floyd, M., Cakir, Z., Doğan, U., et al. (2014). Istanbul's earthquake hot spots: Geodetic constraints on strain accumulation along faults in the Marmara seismic gap. *Geophysical Research Letters*, *41*, 5783–5788. https://doi.org/10.1002/2014GL060985

Flérit, F., Armijo, R., King, G., & Meyer, B. (2004). The mechanical interaction between the propagating North Anatolian Fault and the back-arc extension in the Aegean. *Earth and Planetary Science Letters*, *224*(3), 347–362.

Flerit, F., Armijo, R., King, G. C. P., Meyer, B., & Barka, A. (2003). Slip partitioning in the Sea of Marmara pull-apart determined from GPS velocity vectors. *Geophysical Journal International*, *154*(1), 1–7.

Gökaşan, E., Tur, H., Ergin, M., Görüm, T., Batuk, F. G., Sağcı, N., et al. (2010). Late Quaternary evolution of the Çanakkale Strait region (Dardanelles, NW Turkey): Implications of a major erosional event for the postglacial Mediterranean-Marmara Sea connection. *Geo-Marine Letters*, *30*(2), 113–131.

Görür, N., & Okay, A. I. (1996). A fore-arc origin for the Thrace Basin, NW Turkey. *Geologische Rundschau*, *85*(4), 662–668.

Grall, C., Henry, P., Tezcan, D., de Lepinay, B. M., Bécel, A., Géli, L., et al. (2012). Heat flow in the Sea of Marmara Central Basin: Possible implications for the tectonic evolution of the North Anatolian Fault. *Geology*, *40*(1), 3–6.

Grall, C., Henry, P., Thomas, Y., Westbrook, G. K., Çağatay, M. N., Marsset, B., et al. (2013). Slip rate estimation along the western segment of the Main Marmara Fault over the last 405–490 ka by correlating mass transport deposits. *Tectonics*, *32*, 1587–1601. https://doi.org/10.1002/2012TC003255

Hsü, K. J., Cita, M. B., & Ryan, W. B. F. (1973). The origin of the Mediterranean evaporites. In W. B. F. Ryan, et al. (Eds.), *Leg 13*, *Initial Reports of the Deep Sea Drilling Project* (Vol. 13, pp. 1203–1231). Washington, DC: U.S. Government Printing Office.

Hubert-Ferrari, A., Armijo, R., King, G., Meyer, B., & Barka, A. (2002). Morphology, displacement, and slip rates along the North Anatolian Fault, Turkey. *Journal of Geophysical Research*, *107*(B10), 2235. https://doi.org/10.1029/2001JB000393

Hubert-Ferrari, A., King, G., Manighetti, I., Armijo, R., Meyer, B., & Tapponnier, P. (2003). Long-term elasticity in the continental lithosphere; modelling the Aden ridge propagation and the Anatolian extrusion process. *Geophysical Journal International*, *153*(1), 111–132.

Imren, C., Le Pichon, X., Rangin, C., Demirbağ, E., Ecevitoğlu, B., & Görür, N. (2001). The North Anatolian Fault within the Sea of Marmara: A new interpretation based on multi-channel seismic and multi-beam bathymetry data. *Earth and Planetary Science Letters*, *186*(2), 143–158.

Kahle, H. G., Straub, C., Reilinger, R., McClusky, S., King, R., Hurst, K., et al. (1998). The strain rate field in the eastern Mediterranean region, estimated by repeated GPS measurements. *Tectonophysics*, *294*, 237–252.

Koçyiğit, A. (1989). Basic geological characteristics and total offset of North Anatolian Fault zone in Susehri area, Ne Turkey. *Middle East Technical University, Journal of Pure and Applied Sciences*, *22*, 43–46.

Kurt, H., Sorlien, C. C., Seeber, L., Steckler, M. S., Shillington, D. J., Cifci, G., et al. (2013). Steady late quaternary slip rate on the Cinarcik section of the North Anatolian Fault near Istanbul, Turkey. *Geophysical Research Letters*, *40*, 4555–4559. https://doi.org/10.1002/grl.50882

Laigle, M., Becel, A., de Voogd, B., Hirn, A., Taymaz, T., & Ozalaybey, S. (2008). A first deep seismic survey in the sea of Marmara: Deep basins and whole crust architecture and evolution. *Earth and Planetary Science Letters*, *270*(3), 168–179.

Le Pichon, X., Chamot-Rooke, N., Rangin, C., & Sengör, A. M. C. (2003). The North Anatolian Fault in the Sea of Marmara. *Journal of Geophysical Research*, *108*(B4), 2179. https://doi.org/10.1029/2002JB001862

Le Pichon, X., Şengör, A. C., Kende, J., İmren, C., Henry, P., Grall, C., & Karabulut, H. (2016). Propagation of a strike-slip plate boundary within an extensional environment: The westward propagation of the North Anatolian Fault. *Canadian Journal of Earth Sciences*, *53*(11), 1416–1439.

Le Pichon, X., Şengör, A. M. C., Demirbağ, E., Rangin, C., Imren, C., Armijo, R., et al. (2001). The active Main Marmara Fault. *Earth and Planetary Science Letters*, *192*(4), 595–616.

Manzi, V., Gennari, R., Hilgen, F., Krijgsman, W., Lugli, S., Roveri, M., & Sierro, F. J. (2013). Age refinement of the Messinian Salinity Crisis onset in the Mediterranean. *Terra Nova*, *25*, 315–322.

McClay, K., & Bonora, M. (2001). Analog models of restraining stepovers in strike-slip fault systems. *AAPG Bulletin*, *85*(2), 233–260.

McClusky, S., Balassanian, S., Barka, A., Demir, C., Ergintav, S., Georgiev, I., et al. (2000). Global Positioning System constraints on plate kinematics and dynamics in the eastern Mediterranean and Caucasus. *Journal of Geophysical Research*, *105*(B3), 5695–5719.

Melinte-Dobrinescu, M. C., Suc, J.-P., Clauzon, G., Popescu, S.-M., Armijo, R., Meyer, B., et al. (2009). The Messinian Salinity Crisis in the Dardanelles region: Chronostratigraphic constraints. *Palaeogeography, Palaeoclimatology, Palaeoecology*, *278*(1), 24–39.

Okay, A. I., Demirbağ, E., Kurt, H., Okay, N., & Kuşçu, İ. (1999). An active, deep marine strike-slip basin along the North Anatolian fault in Turkey. *Tectonics*, *18*(1), 129–147.

Okay, A. I., Kaşlılar-Özcan, A., Imren, C., Boztepe-Güney, A., Demirbağ, E., & Kuşçu, İ. (2000). Active faults and evolving strike-slip basins in the Marmara Sea, northwest Turkey: A multichannel seismic reflection study. *Tectonophysics*, *321*(2), 189–218.

Okay, A. I., Tüysüz, O., & Kaya, Ş. (2004). From transpression to transtension: Changes in morphology and structure around a bend on the North Anatolian Fault in the Marmara region. *Tectonophysics*, *391*(1), 259–282.

Okay, A. I., Zattin, M., & Cavazza, W. (2010). Apatite fission-track data for the Miocene Arabia-Eurasia collision. *Geology*, *38*(1), 35–38.

Önal, M. (1984). Gelibolu (Çanakkale) kuzeybatısının jeolojisi: I. Ü. Fen Bilimleri Enstitüsü. (PhD thesis, 200 pp.).

Parke, J., Minshull, T., Anderson, G., White, R., McKenzie, D., Kuscu, I., et al. (1999). Active faults in the Sea of Marmara, western Turkey, imaged by seismic reflection profiles. *Terra Nova*, *11*, 223–227.

Popescu, S.-M., Melinte-Dobrinescu, M. C., Suc, J.-P., & Do Couto, D. (2017). *Ceratolithus acutus* Gartner and Bukry 1974 (= *C. armatus* Müller 1974), calcareous nannofossil marker of the marine reflooding that terminated the Messinian Salinity Crisis: Comment on "*Paratethyan ostracods in the Spanish Lago-Mare: More evidence for interbasinal exchange at high Mediterranean Sea level*" by Stoica et al., *Palaeogeogr., Palaeoclimatol., Palaeoecol.*, 441, 854-870. *Palaeogeography, Palaeoclimatology, Palaeoecology*, 485, 986-989.

Raffi, I., Backman, J., Fornaciari, E., Pälike, H., Rio, D., Lourens, L., & Hilgen, F. (2006). A review of calcareous nannofossil astrobiochronology encompassing the past 25 million years. *Quaternary Science Reviews*, *25*(23), 3113–3137.

Rangin, C., Le Pichon, X., Demirbag, E., & Imren, C. (2004). Strain localization in the Sea of Marmara: Propagation of the North Anatolian Fault in a now inactive pull-apart. *Tectonics*, *23*, TC2014. https://doi.org/10.1029/2002TC001437

Rangin, C., Demirbag, E., Imren, C., Crusson, A., Normand, A., Le Drezen, E., & Le Bot, A. (2001). Marine Atlas of the Sea of Marmara (Turkey), 11 plates and 1 booklet, Special publication by Ifremer Brest Technology Center, France.

Roberts, A. P. (1995). Tectonic rotation about the termination of a major strike-slip fault, Marlborough fault system, New Zealand. *Geophysical Research Letters*, *22*(3), 187–190.

Roveri, M., Flecker, R., Krijgsman, W., Lofi, J., Lugli, S., Manzi, V., et al. (2014). The Messinian Salinity Crisis: Past and future of a great challenge for marine sciences. *Marine Geology*, *352*, 25–58.

Sakınç, M., Yaltırak, C., & Oktay, F. Y. (1999). Palaeogeographical evolution of the Thrace Neogene Basin and the Tethys–Paratethys relations at northwestern Turkey (Thrace). *Palaeogeography, Palaeoclimatology, Palaeoecology*, *153*(1), 17–40.

Saner, S. (1980). Batı Pontidler'in ve komşu havzaların oluşumlarının levha tektoniği kuramıyla açıklanması, Kuzeybatı Türkiye. *Maden Tetkik ve Arama Dergisi*, *93*(93), 94.

Seeber, L., Emre, O., Cormier, M. H., Sorlien, C. C., McHugh, C. M. G., Polonia, A., et al. (2004). Uplift and subsidence from oblique slip: The Ganos–Marmara bend of the North Anatolian Transform, western Turkey. *Tectonophysics*, *391*(1), 239–258.

Şengör, A. M. C., Görür, N., & Şaroğlu, F. (1985). Strike-slip faulting and related basin formation in zones of tectonic escape: Turkey as a case study. In K. T. Biddle & N. Christie-Blick (Eds.), *Strike-slip faulting and Basin formation. Society of Economic Paleontologists and Mineralogist, Special Publication* (pp. 227–267).

Şengör, A. M. C., Tüysüz, O., İmren, C., Sakınç, M., Eyidoğan, H., Görür, N., et al. (2005). The North Anatolian Fault: A new look. *Annual Review of Earth and Planetary Sciences*, *33*, 37–112.

Şengör, A. M. C., & Yılmaz, Y. (1981). Tethyan evolution of Turkey: A plate tectonic approach. *Tectonophysics*, *75*(3), 181–241.

Şentürk, K., & Okay, A. I. (1984). Blueschists discovered east of Saros Bay in Thrace. *Bulletin of the Mineral Research and Exploration Institute (MTA) of Turkey*, *97*(98), 72–75.

Sternai, P., Jolivet, L., Menant, A., & Gerya, T. (2014). Driving the upper plate surface deformation by slab rollback and mantle flow. *Earth and Planetary Science Letters*, *405*, 110–118.

Suc, J. P., Popescu, S. M., Do Couto, D., Clauzon, G., Rubino, J. L., Melinte-Dobrinescu, M. C., et al. (2015). Marine gateway vs. fluvial stream within the Balkans from 6 to 5 Ma. *Marine and Petroleum Geology*, *66*, 231–245.

Sümengen, M., & Terlemez, I. (1991). Güneybati Trakya yöresi Eosen çökelleri stratigrafisi. *MTA Dergisi*, *113*, 17–30.

Tapponnier, P., Peltzer, G., Le Dain, A. Y., Armijo, R., & Cobbold, P. (1982). Propagating extrusion tectonics in Asia: New insights from simple experiments with plasticine. *Geology*, *10*(12), 611–616.

Titus, S. J., Housen, B., & Tikoff, B. (2007). A kinematic model for the Rinconada fault system in central California based on structural analysis of en echelon folds and paleomagnetism. *Journal of Structural Geology*, *29*(6), 961–982.

Turgut, S., Türkaslan, M., & Perinçek, D. (1991). Evolution of the Thrace sedimentary basin and its hydrocarbon prospectivity. *Generation, accumulation, and Production of Europe's hydrocarbons*, *1*, 415–437.

Türkecan, A., & Yurtsever, A. (2002). Geological map of Turkey at 1/500.000: Istanbul. Maden Tetkik ve Arama Genel Müdürlüğü, Ankara.

Tüysüz, O., Barka, A., & Yiğitbaş, E. (1998). Geology of the Saros graben and its implications for the evolution of the North Anatolian Fault in the Ganos–Saros region, northwestern Turkey. *Tectonophysics*, *293*(1), 105–126.

Walcott, R. I. (1978). Present tectonics and late Cenozoic evolution of New Zealand. *Geophysical Journal International*, *52*(1), 137–164.

Wilcox, R. E., Harding, T. T., & Seely, D. R. (1973). Basic wrench tectonics. *AAPG Bulletin*, *57*(1), 74–96.

Wong, H. K., Lüdmann, T., Ulug, A., & Görür, N. (1995). The Sea of Marmara: A plate boundary sea in an escape tectonic regime. *Tectonophysics*, *244*(4), 231–250.

Wright, T., Parsons, B., & Fielding, E. (2001). Measurement of interseismic strain accumulation across the North Anatolian Fault by satellite radar interferometry. *Geophysical Research Letters*, *28*(10), 2117–2120.

Yaltırak, C. (1996). Ganos Fay Sistemi'nin tektonik tarihi. *TPJD Bülteni*, *S 8*(1), 137–156.

Yaltırak, C., Mehmet, S., & Oktay, F. Y. (2000). Westward propagation of north Anatolian fault into the northern Aegean: Timing and kinematics: Comment and reply comment. *Geology*, *28*(2), 187–188.

Yılmaz, Y., & Clift, P. D. (1990). Allochthonous terranes in the Tethyan Middle East: Anatolia and the surrounding regions [and discussion]. *Philosophical Transactions of the Royal Society of London A: Mathematical, Physical and Engineering Sciences*, *331*(1620), 611–624.

Yılmaz, Y., Tüysüz, O., Yiğitbaş, E., Genc, S. C., & Şengör, A. M. C. (1997). AAPG memoir 68: Regional and petroleum geology of the Black Sea and surrounding region. Chapter 11: Geology and Tectonic Evolution of the Pontides: 183-226.

Zattin, M., Cavazza, W., Okay, A. I., Federici, I., Fellin, M. G., Pignalosa, A., & Reiners, P. (2010). A precursor of the North Anatolian Fault in the Marmara Sea region. *Journal of Asian Earth Sciences*, *39*(3), 97–108.

Zattin, M., Okay, A. I., & Cavazza, W. (2005). Fission-track evidence for late Oligocene and mid-Miocene activity along the North Anatolian Fault in south-western Thrace. *Terra Nova*, *17*(2), 95–101.